

Uptake of nitric acid in ice crystals in persistent contrails

D. Schäuble^{*}, C. Voigt, B. Kärcher, P. Stock, H. Schlager

Deutsches Zentrum für Luft- und Raumfahrt, Institut für Physik der Atmosphäre, Oberpfaffenhofen, Germany

M. Krämer, C. Schiller, R. Bauer, N. Spelten

Institut für Stratosphärenforschung, FZ Jülich, Jülich, Germany

M. de Reus, M. Szakáll, S. Borrmann

Institut für Physik der Atmosphäre, Johannes-Gutenberg Universität Mainz, Mainz, Germany

U. Weers, T. Peter

Institut für Atmosphäre und Klima, ETH Zürich, Zürich, Switzerland

Keywords: Nitric acid, Partitioning, Uptake, Contrails, Cirrus

ABSTRACT: This is a short version of Schäuble et al. (2009) published in ACPD. In November 2006 cirrus clouds and almost 40 persistent contrails were probed with in situ instruments over Germany and Northern Europe during the CIRRUS-III campaign. At altitudes between 10 and 11.5 km and temperatures of 211 to 220 K contrails with ages up to 8 hours were detected. These contrails had a larger ice phase fraction of total nitric acid ($\text{HNO}_{3,\text{ice}}/\text{HNO}_{3,\text{tot}} = 6\%$) than the ambient cirrus layers (3%). The differences in ice phase fractions between developing contrails and cirrus are likely caused by high plume concentrations of HNO_3 prior to contrail formation and large ice crystal number densities in contrails. The observed decrease of nitric acid to water molar ratios in ice with increasing mean ice particle diameter suggests that ice-bound HNO_3 concentrations are controlled by uptake of exhaust HNO_3 in the freezing plume aerosol in young contrails and subsequent trapping of ambient HNO_3 in growing ice particles in older (age > 1 h) contrails.

1 INTRODUCTION

In the tropopause region the ozone budget is influenced by heterogeneous processes such as the uptake of nitric acid (HNO_3) in cirrus clouds. Results from a global chemistry transport model indicate that HNO_3 uptake in cirrus ice particles and subsequent particle sedimentation has the potential to remove HNO_3 irreversibly from this region, leading to a large-scale reduction of gas phase HNO_3 concentrations (von Kuhlmann and Lawrence, 2006). At typical upper tropospheric NO_x levels the irreversible removal of gaseous HNO_3 reduces the concentrations of the ozone precursor nitrogen oxide ($\text{NO}_x = \text{NO} + \text{NO}_2$) and thus net ozone production rates. Reductions in local ozone concentrations of up to 14% are found in chemistry box model studies (Meier and Hendricks, 2002).

During several field campaigns from the tropics to the Arctic the interaction of HNO_3 and cirrus ice crystals was experimentally investigated (e.g. Weinheimer et al., 1998; Popp et al., 2004; Voigt et al., 2006). Voigt et al. (2006) summarized these measurements in terms of average nitric acid to water molar ratios ($\mu = \text{HNO}_{3,\text{ice}}/\text{H}_2\text{O}_{\text{ice}}$) in cirrus ice particles and ice-bound fractions of total nitric acid ($\Phi = \text{HNO}_{3,\text{ice}}/\text{HNO}_{3,\text{tot}}$). Kärcher and Voigt (2006) explained the inverse temperature trend of the μ and Φ data by means of a model describing nitric acid uptake in growing ice crystals (trapping).

Simulations by Kärcher et al. (1996) indicate the formation of high levels of HNO_3 in jet aircraft exhaust plumes prior to contrail formation. E.g. Arnold et al. (1992) measured gas phase HNO_3 in young aircraft plumes. The efficient transfer of gaseous HNO_3 into plume aerosols and ice particles during contrail formation is demonstrated by Kärcher (1996) by means of microphysical simulations. Gao et al. (2004) measured HNO_3 in ice particles of a WB-57 aircraft contrail in the subtrop-

^{*} *Corresponding author:* Dominik Schäuble, Deutsches Zentrum für Luft- und Raumfahrt (DLR) – Institut für Physik der Atmosphäre, Oberpfaffenhofen, D-82234 Wessling, Germany. Email: dominik.schaeuble@dlr.de

ics at 14 – 15 km altitude. They observed HNO₃ in contrail particles at temperatures below 205 K, presumably in the form of NAT, but did not explicitly report ice phase HNO₃ concentrations.

An experimental quantification of the HNO₃ content in contrail ice particles as a function of mean ice particle size, a proxy for the microphysical age of persistent contrails, is lacking. So our observations provide an unprecedented data set on the uptake of HNO₃ in persistent contrails.

2 INSTRUMENTATION

During the CIRRUS-III campaign in November 2006, the Enviscope Learjet performed 5 flights at latitudes between 48°N and 68°N with instruments measuring NO_y, H₂O, small ice crystal size distributions, and condensation nuclei (CN). Total and gas phase NO_y were measured based on the chemiluminescence technique with a forward- and a backward-facing inlet, respectively. We calculated the concentration of particulate (in our case essentially ice phase) reactive nitrogen, $\text{NO}_{y,\text{ice}} = (\text{NO}_{y,\text{forw}} - \text{NO}_{y,\text{back}}) / \text{EF}_{\text{NO}_y}$, in contrails with a size-dependent relationship for the enhancement factor $\text{EF}_{\text{NO}_y}(d)$ (Belyaev and Levin, 1974). Nitric acid was directly measured during the flight on 28 November (nylon filter technique). The HNO₃ concentration on 24 and 29 November was derived from NO_y observations and the HNO₃ to NO_y ratio (0.45 ± 0.2) detected on 28 November. This ratio is in good agreement with previous observations in midlatitudes (e.g. Talbot et al., 1999).

In young contrails NO_x constitutes the major fraction of NO_y. A microphysical plume model study (Meilinger et al., 2005) including detailed heterogeneous aerosol and ice phase chemistry indicates that the chemical conversion into HNO₃ is small in contrails in terms of the gas phase HNO₃/NO_y ratio ($\approx 1\%$) within the first ten hours after emission due to heterogeneous dehydroxylation and production of HONO. In such contrails the gas phase HNO₃ concentration is supposed to be controlled by entrainment of ambient HNO₃. Thus, we used the ambient HNO₃ concentration as an approximation for the concentration inside contrails. In cirrus clouds as well as in contrails, HNO₃ is assumed to account for 100 % of NO_y in ice particles. The uptake of PAN and HONO on ice crystals is probably small compared to HNO₃ (Bartels-Rausch et al., 2002) and N₂O₅ and HO₂NO₂ are quickly photolyzed during daytime.

Total water was measured with the forward-facing inlet of the Fast In situ Stratospheric Hygrometer (FISH) (Zöger et al., 1999) and water vapour was detected with a TDL instrument (OJSTER). The Forward Scattering Spectrometer Probe FSSP-100 (Borrmann et al., 2000) measured the number concentration and size distribution of particles with diameters of 2.8 – 29.2 μm.

Contrails were identified from distinct simultaneous short-term increases in the time series of the concentrations of NO_{y,gas}, NO_{y,tot}, CN (> 5 nm diameter, not discussed here), and ice particles. Lower limits of 0.1 nmol/mol for $\Delta\text{NO}_{y,\text{gas}}$ and 100 cm⁻³ for ΔCN enabled a separation of contrails from cirrus clouds that were not affected by aviation within the last 8 h of their lifetime. Contrails often exhibit significant spatial inhomogeneities in structure and dilution properties. The spatially random sampling of contrails and merging of several individual contrails introduce considerable uncertainty in the exact determination of contrail age from plume dilution data which is difficult to quantify.

3 NITRIC ACID PARTITIONING AND ICE WATER CONTENT IN CONTRAILS

European Centre for Medium-Range Weather Forecasts analyses indicate that the top regions of frontal cirrus layers were probed on 24 and 29 November, whereas on 28 November the observations originate from deeper inside cirrus clouds. Figure 1 shows a typical time series of data from the flight on 24 November over Germany.

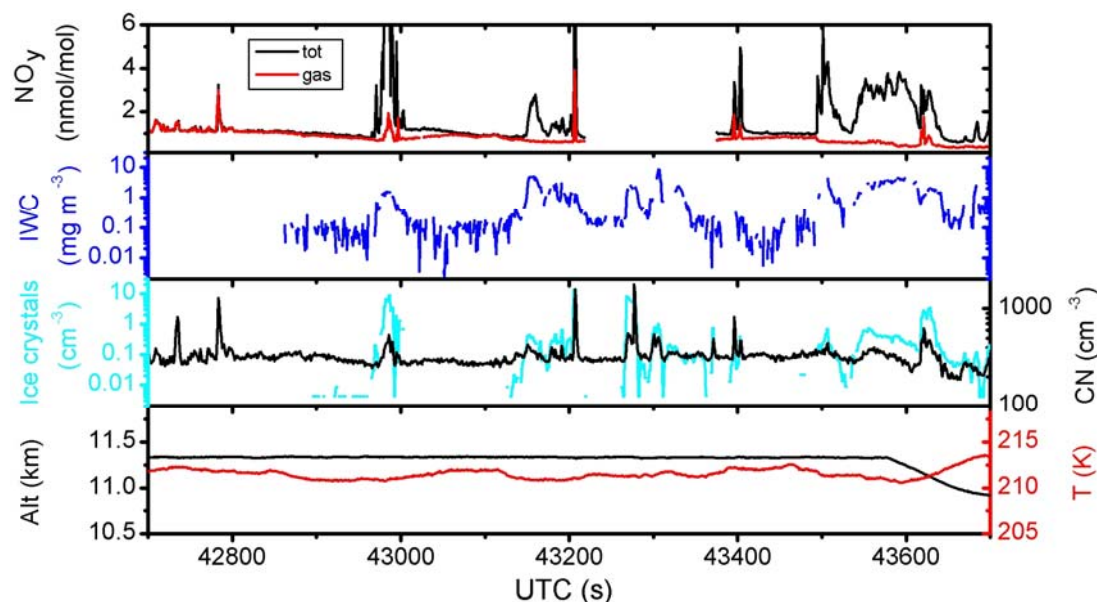


Figure 1. Time series of gas phase and total NO_y , ice water content (IWC), number densities of ice particles with approximate diameters between 2.8 and 29.2 μm , CN ($> 5\text{nm}$) concentration, as well as altitude and temperature for a period of the flight on 24 November 2006. Exhaust plume at 42,780 s, contrails at approximately 42,980 s, 43,200 s, 43,400 s, and 43,620 s, and cirrus clouds around 43,150 s and 43,550 s. Gaps in the NO_y measurements are due to calibration procedures.

On average, contrails were found to have larger Φ values than the cirrus layers under similar conditions. This is illustrated by means of the probability density function of Φ (Fig. 2a). At temperatures between 211 and 220 K, contrail ice particles contained on average 6 % (cirrus 3 %) of the total nitric acid.

Twelve young contrails with $\Delta\text{NO}_{y,\text{gas}} > 0.75$ nmol/mol, corresponding to ages $< 1\text{h}$, had even larger ice phase nitric acid fractions (9 %). The maximum Φ measured in contrails was 22 %. The gas phase equivalent mixing ratio of nitric acid in ice, $\text{HNO}_{3,\text{ice}}$, is 14 pmol/mol in contrails compared to 6 pmol/mol in the cirrus layers. The mean $\text{HNO}_{3,\text{ice}}$ in the young contrails is 21 pmol/mol.

Figure 2b (top panel) shows the temperature dependence of the ice phase molar ratios of nitric acid and water (μ) in contrails (red circles) and in the surrounding cirrus layers (grey circles) that were not recently influenced by aviation. The μ values generally increase with decreasing temperature, as the probability of HNO_3 molecules to escape from the growing ice surfaces after adsorption is reduced at low temperatures leading to more efficient trapping of HNO_3 (Kärcher and Voigt, 2006).

The curves are results from the trapping model by Kärcher et al. (2009). The dashed and solid model curves were computed for HNO_3 partial pressures of 3×10^{-8} hPa and 6×10^{-8} hPa, respectively, roughly capturing the range of measured values occurring in contrails and cirrus (see above). The trapping model bounds the observed mean μ values in cirrus (black squares) very well at 211–220 K. The model assumes temperature-dependent mean ice particle growth rates (net supersaturations) to estimate steady-state molar ratios. Deviations of individual data points from the mean model curves are likely caused by variable growth/sublimation histories of the observed ice particles. Further, the μ of small ice crystals may be strongly influenced by the composition of the freezing aerosol resulting in values exceeding the means (Sect. 4). The mean $\text{HNO}_3/\text{H}_2\text{O}$ molar ratio in contrails of 4×10^{-6} is found to be approximately twice as large as in the cirrus layers (2×10^{-6}).

Figure 2b (bottom panel) illustrates the IWC of contrails and cirrus clouds versus temperature. The difference between the CIRRUS-III IWCs and the climatological means (solid curve) by Schiller et al. (2008) are discussed in Schäuble et al. (2009). The contrails have a slightly larger mean IWC (red squares) than the cirrus clouds, 1.8 and 1.3 mg m^{-3} , respectively. The IWC of young contrails 2.9 mg m^{-3} is more than twice the cirrus mean. The H_2O aircraft emissions become unimportant for contrails older than a few minutes, according to plume dilution estimates (Gerz et al., 1998). Differences between contrail and cirrus IWCs are expected to diminish over time as most of the H_2O in contrail ice condenses from the ambient air during ice particle growth.

We additionally report a striking difference between measured contrail and cirrus cloud ice particle number densities in the FSSP-100 size range 2.8–29.2 μm in diameter, 1.5 cm^{-3} and 0.21 cm^{-3} ,

respectively. Figure 3a shows the increase of the ice-bound nitric acid fraction with increasing ice crystal number densities in contrails (means in black). Together this is one explanation for the larger Φ in contrails compared to cirrus.

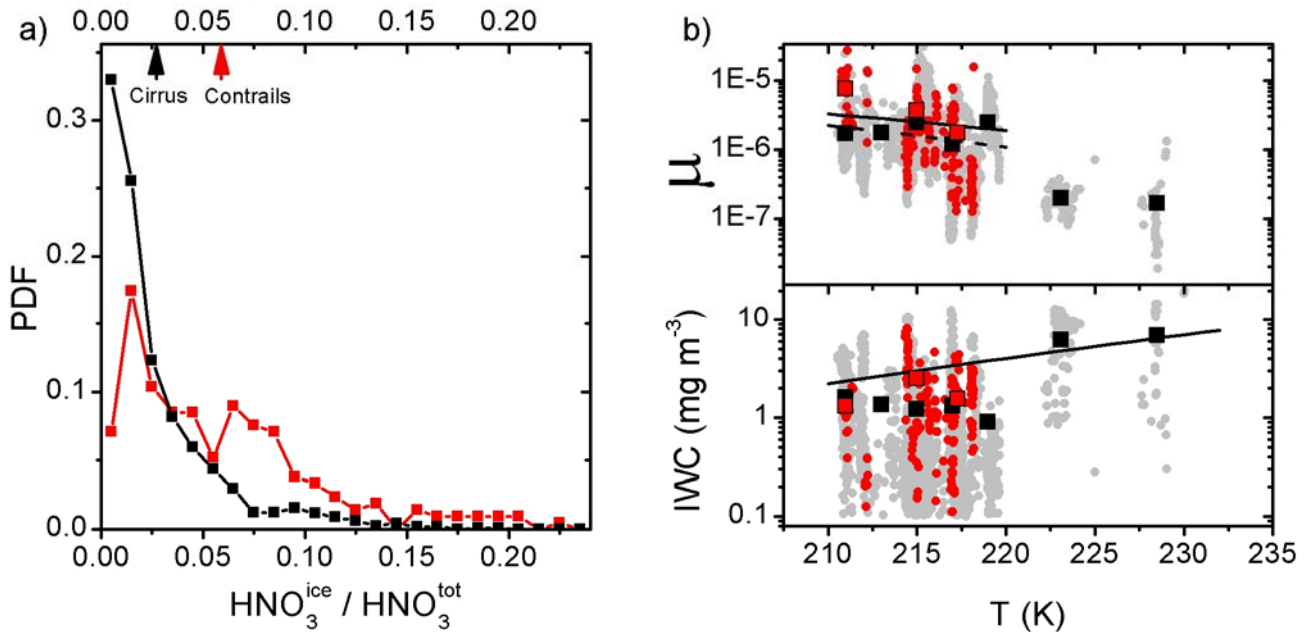


Figure 2. a) Normalized probability density function of the ice phase fraction of total HNO_3 , Φ , for contrails (red) and cirrus clouds (black). Arrows indicate the means for the temperature range (211 – 220 K) where contrails occurred. b) The temperature dependence of the (top) molar ratio of nitric acid to water in ice particles ($\mu = \text{HNO}_{3,\text{ice}}/\text{H}_2\text{O}_{\text{ice}}$) and (bottom) ice water content (IWC) of contrails (red circles) and cirrus clouds (grey circles). Squares are means over 2 K temperature bins. Curves are model results, see text for details. The curve in the bottom panel depicts the mean cirrus IWCs based on a large number of in situ measurements at midlatitudes (Schiller et al., 2008).

4 NITRIC ACID UPTAKE IN DEVELOPING CONTRAILS

Given the limited amount of contrail data, it is unclear whether the systematic differences in ice phase fraction and molar ratios in ice presented in Section 3 are representative. Nevertheless, sorting the molar ratio data as a function of the mean ice particle size enables us to study the HNO_3 uptake process in contrails in more detail.

Figure 3b shows the molar ratios (grey circles) along with the mean (black squares) and median (grey squares) values of the contrails probed during CIRRUS-III as a function of the mean ice particle diameter. We associate rough estimates of the contrail age with the mean diameter based on the gas phase ΔNO_y data (Schumann et al., 1998), as indicated in the figure. In persistent contrails, the mean size increases due primarily to uptake of H_2O from the gas phase (depositional growth). The measurements show a clear trend of decreasing μ with increasing mean size or age. Young contrails with ages 10 – 15 min and mean diameters 7 μm have a mean $\mu \approx 10^{-5}$, while older contrails with ages > 1 h and mean diameters > 10 – 15 μm exhibit values closer to the mean 2×10^{-6} of the cirrus data. How are the high molar ratios in young contrails brought about? We argue that a high concentration of HNO_3 entered the ice particles already during contrail formation, when they are very small (mean diameters 1 μm), leading to very high molar ratios. Subsequent depositional growth increases the size per ice particle, while trapping in young contrails (mean diameters 1 – 10 μm) only adds a small contribution to the HNO_3 content per particle; both effects cause μ to decrease in this phase of contrail development. Further growth to larger sizes diminishes the role of the initially high molar ratios and trapping takes over the dominant part in determining μ . These processes are illustrated by the model curves as explained in detail in Schäuble et al. (2009).

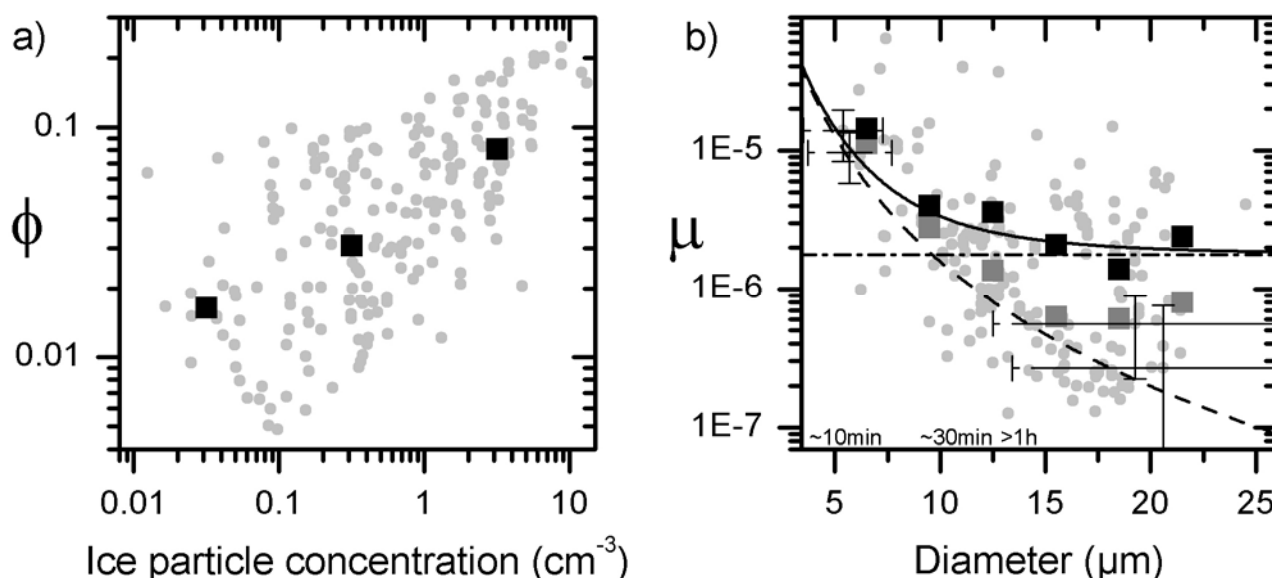


Figure 3. a) Ice-bound nitric acid fraction versus ice crystal number density for mean ice particle diameters between 2.8 and 29.2 μm . b) Molar ratios of nitric acid to water in contrail ice particles μ versus mean ice particle diameter. A detailed description is given in Schäuble et al. (2009).

5 SUMMARY AND CONCLUSIONS

During the CIRRUS-III field campaign gas phase and ice phase reactive nitrogen, ice water content, and ice crystal size distributions were measured in contrails and cirrus at midlatitudes close to the tropopause. The temperatures and HNO_3 partial pressures were in the ranges 210 – 230 K and $3 - 6 \times 10^{-8}$ hPa, respectively. The observed uptake of HNO_3 in ice particles residing in the top layers of frontal cirrus clouds confirms previous results from airborne field campaigns carried out in polar, midlatitude, and sub-tropical regions (Voigt et al., 2006).

On average the probed contrails contained twice as much ice-bound HNO_3 as the cirrus clouds within 211 – 220 K, 14 pmol/mol and 6 pmol/mol, respectively. Thus, the mean fraction of total HNO_3 in ice particles was considerably larger in the contrails (6 %) than in the cirrus layers (3 %). In young contrails (approximate age < 1 h) this fraction was even higher (9 %). The measured molar ratios of HNO_3 and H_2O in contrail ice particles exceeded 10^{-5} for small particle sizes, or contrail ages. For older contrails, molar ratios approached the mean value of 2×10^{-6} detected in the cirrus layers. Averaged over all detected contrails regardless of age, this caused the mean molar ratios in contrails to be about twice as large as in the cirrus clouds.

Motivated by our study, contrails may be regarded as an atmospheric laboratory to study HNO_3 uptake during ice particle growth. Our data show that ice phase $\text{HNO}_3/\text{H}_2\text{O}$ molar ratios decrease during contrail ageing. This dependence was explained by uptake of high levels of HNO_3 into the freezing aerosol particles during ice formation in contrails and subsequent trapping of relatively low levels of ambient HNO_3 in growing contrail ice particles. In young contrails with ages < 1 h or mean diameters < 10 μm , the ice phase HNO_3 concentrations are therefore largely controlled by the jet engine NO_x and OH emission indices. More airborne measurements with extended instrumentation are needed to study the dependence of HNO_3 uptake on HNO_3 partial pressure and to better quantify ice particle size distributions in developing contrails.

The results of this study help constrain chemical-microphysical models simulating heterogeneous chemistry in persistent contrails in order to constrain the impact of plume processing of NO_x emissions on the chemical production or loss of ozone.

REFERENCES

- Arnold, F., J. Scheid, T. Stimp, H. Schlager, and M.E. Reinhardt, 1992: Measurements of jet aircraft emissions at cruise altitude I: the odd-nitrogen gases NO , NO_2 , HNO_2 and HNO_3 , *Geophys. Res. Lett.*, 19, 2421 - 2424.

- Bartels-Rausch, T., B. Eichler, P. Zimmermann, H. W. Gäggeler, and M. Ammann, 2002: The adsorption of nitrogen oxides on crystalline ice, *Atmos. Chem. Phys.*, *2*, 235 - 247.
- Belyaev, S.P. and L. M. Levin, 1974: Techniques for collection of representative aerosol samples, *J. Aerosol Sci.*, *5*, 325 - 338.
- Borrmann, S., B. P. Luo, and M. Mishchenko, 2000: Application of the T-matrix method to the measurement of aspherical (ellipsoidal) particles with forward scattering optical particle counters, *J. Aerosol Sci.*, *31*, 789 - 799.
- Gao, R. S., P. J. Popp, D. W. Fahey, T. P. Marcy, R. L. Herman, E. M. Weinstock, D. Baumgardner, T. J. Garrett, K. H. Rosenlof, T. L. Thompson, T. P. Bui, B. A. Ridley, S. C. Wofsy, O. B. Toon, M. A. Tolbert, B. Kärcher, T. Peter, P. K. Hudson, A. J. Weinheimer, and A. J. Heymsfield, 2004: Evidence that nitric acid increases relative humidity in low-temperature cirrus clouds, *Science*, *303*, 516 - 520.
- Gerz, T., T. Dürbeck, and P. Konopka, 1998: Transport and effective diffusion of aircraft emissions, *J. Geophys. Res.*, *103*, 25905 - 25913.
- Kärcher, B., 1996: Aircraft-generated aerosols and visible contrails, *Geophys. Res. Lett.*, *23*, 1933 - 1936.
- Kärcher, B. and C. Voigt, 2006: Formation of nitric acid/water ice particles in cirrus clouds, *Geophys. Res. Lett.*, *33*, L08806, doi10.1029/2006GL025927.
- Kärcher, B., M. M. Hirschberg, and P. Fabian, 1996: Small-scale chemical evolution of aircraft exhaust species at cruising altitudes, *J. Geophys. Res.*, *101*, 15169 - 15190.
- Kärcher, B., J. P. D. Abbatt, R. A. Cox, P. J. Popp, and C. Voigt, 2009: Trapping of trace gases by growing ice surfaces including surface-saturated adsorption, *J. Geophys. Res.*, *114*, D13306, doi:10.1029/2009JD011857.
- Meier, A. and J. Hendricks, 2002: Model studies on the sensitivity of upper tropospheric chemistry to heterogeneous uptake of HNO₃ on cirrus ice particles, *J. Geophys. Res.*, *107*, 4696, doi10.1029/2001JD000735.
- Meilinger, S. K., B. Kärcher, and Th. Peter, 2005: Microphysics and heterogeneous chemistry in aircraft plumes - high sensitivity on local meteorology and atmospheric composition, *Atmos. Chem. Phys.*, *5*, 533 - 545, 2005.
- Popp, P.J., R. S. Gao, T. P. Marcy, D. W. Fahey, P. K. Hudson, T. L. Thompson, B. Kärcher, B. A. Ridley, A. J. Weinheimer, D. J. Knapp, D. D. Montzka, D. Baumgardner, T. J. Garrett, E. M. Weinstock, J. B. Smith, D. S. Sayres, J. V. Pittman, S. Dhaniyala, T. P. Bui, and M. J. Mahoney, 2004: Nitric acid uptake on subtropical cirrus cloud particles, *J. Geophys. Res.*, *109*, D06302, doi10.1029/2003JD004255.
- Schäuble, D., C. Voigt, B. Kärcher, P. Stock, H. Schlager, M. Krämer, C. Schiller, R. Bauer, N. Spelten, M. de Reus, M. Szakáll, S. Borrmann, U. Weers, T. Peter, 2009: Airborne measurements of the nitric acid partitioning in persistent contrails, *Atmos. Chem. Phys. Discuss.*, *9*, 1 - 22.
- Schiller, C., M. Krämer, A. Afchine, N. Spelten, and N. Sitnikov, 2008: Ice water content of Arctic, midlatitude, and tropical cirrus, *J. Geophys. Res.*, *113*, D24208, doi10.1029/2008JD010342.
- Schumann, U., H. Schlager, F. Arnold, R. Baumann, P. Haschberger, and O. Klemm, 1998: Dilution of aircraft exhaust plumes at cruise altitudes, *Atmos. Environ.*, *32*, 3097 - 3103.
- Talbot, R.W., J. E. Dibb, E. M. Scheuer, Y. Kondo, M. Koike, H. B. Singh, L. B. Salas, Y. Fukui, J. O. Ballenthin, R. F. Meads, T. M. Miller, D. E. Hunton, A. A. Viggiano, D. R. Blake, N. J. Blake, E. Atlas, F. Flocke, D. J. Jacob, and L. Jaegle, 1999: Reactive nitrogen budget during the NASA SONEX mission, *Geophys. Res. Lett.*, *26*, 3057 - 3060.
- Voigt, C., H. Schlager, H. Ziereis, B. Kärcher, B. P. Luo, C. Schiller, M. Krämer, P. J. Popp, H. Irie, and Y. Kondo, 2006: Nitric acid in cirrus clouds, *Geophys. Res. Lett.*, *33*, L05803, doi10.1029/2005GL025159.
- von Kuhlmann, R. and M. G. Lawrence, 2006: The impact of ice uptake of nitric acid on atmospheric chemistry, *Atmos. Chem. Phys.*, *6*, 225 - 235.
- Weinheimer, A. J., T. L. Campos, J. G. Walega, F. E. Grahek, B. A. Ridley, D. Baumgardner, C. H. Twohy, B. Gandrud, and E. J. Jensen, 1998: Uptake of NO_y on wave-cloud ice particles, *Geophys. Res. Lett.*, *25*, 1725 - 1728.
- Zöger, M., A. Afchine, N. Eicke, M. T. Gerhards, E. Klein, D. S. McKenna, U. Mörschel, U. Schmidt, V. Tan, F. Tuitjer, T. Woyke, and C. Schiller, 1999: Fast in situ stratospheric hygrometers: A new family of balloon-borne and airborne Lyman- α photofragment fluorescence hygrometers, *J. Geophys. Res.*, *104*, 1807 - 1816.